Vibronic Structure in the S_1-S_0 Transition of Jet-Cooled Dibenzofuran

Masaaki Baba* and Koichi Mori

Division of Chemistry, Graduate School of Science, Kyoto University, Kyoto 606-8502, Japan

Michiru Yamawaki, Kumi Akita, Masahide Ito, and Shunji Kasahara

Molecular Photoscience Research Center, Kobe University, Nada-ku, Kobe 657-8501, Japan

Takaya Yamanaka

Laser Research Center for Molecular Science, Institute for Molecular Science, Myodaiji, Okazaki 444-8585, Japan

Received: January 26, 2006; In Final Form: May 22, 2006

Fluorescence excitation spectra of dibenzofuran in a supersonic jet are observed and the vibronic structure is analyzed for the S_1 $^1A_1$ ($\pi\pi^*$) and S_0 states. An observation of the rotational envelopes reveals that the 0_0^0 band is a B-type band. However, it is shown that most of the strong vibronic bands are A-type bands. The intensity arises from vibronic coupling with the S_2 $^1B_2$ state. We find a broad emission in the dispersed fluorescence spectrum for the excitation of the high vibrational levels in the S_1 state. This indicates that intramolecular vibrational redistribution (IVR) occurs efficiently in the isolated dibenzofuran molecule.

Introduction

Dibenzofuran is one of the prototypical molecules of toxic dioxins.[1] This molecule is also interesting from a spectroscopic point of view and many studies have been conducted in the solid state and gas phase.[2−7] Recently, we have observed the rotationally resolved ultrahigh-resolution spectra of the $S_1 \leftarrow S_0$ transition of dibenzofuran in a collimated molecular beam.[8] The isolated dibenzofuran molecule is shown to be planar in both the S_0 and S_1 states by an accurate determination of rotational constants. Furthermore, the 0_0^0 band has been shown to be a B-type band, where the transition moment is along the 2-fold symmetry axis, and the S_1 state has been identified as the $^1A_1$ ($\pi\pi^*$) state. The rotational constants of the S_0 and S_1 states are almost the same. Therefore, it is considered that the stable conformation does not change significantly by electronic excitation. In this case, the 0_0^0 band is generally strong and vibronic bands are relatively weak. However, many vibronic bands are strong in the fluorescence excitation spectrum in a supersonic jet.[9−11] This indicates that the S_1 $^1A_1$ ($\pi\pi^*$) state is remarkably mixed with another excited state by vibronic interaction. In fact, the $0_0^0 + 443$ cm^{-1} band, which is stronger than the 0_0^0 band, is shown to be an A-type band by analyzing the rotationally resolved spectrum. The transition moment is along the long axis of the molecule; this has been previously shown an a polarization study of the polyethylene film.[3]

To elucidate the vibrational structure and the direction of the transition moment for each vibronic band, we have examined high-resolution fluorescence excitation spectrum and the rotational envelopes of prominent vibronic bands in the supersonic jet. The results and analysis are described in this article. We have also observed dispersed fluorescence spectra for the excitation of several vibronic bands. A broad emission is observed when the high vibrational level is excited. We discuss intramolecular vibrational redistribution (IVR) in the S_1 states of the isolated dibenzofuran molecule.

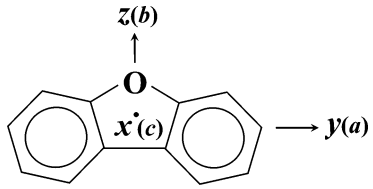

Figure 1. Molecular structure and rotational axes of dibenzofuran.

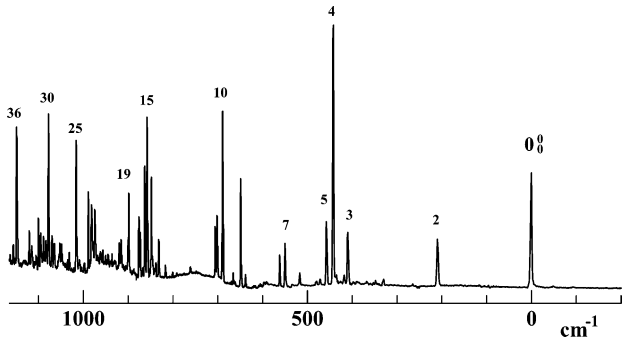

Figure 2. Fluorescence excitation spectrum of dibenzofuran in a supersonic jet.

Experimental Section

Dibenzofuran (Nacalai Tesque) was recrystallized from ethanol and the solid sample was heated to 100 °C in a stainless steel container. The vapor was mixed with Ar gas (3.5 atm) and expanded into a vacuum chamber through a pulsed nozzle (automobile fuel injector, orifice diameter of 0.8 mm) to produce a supersonic jet. The light source was a tunable dye laser (Lambda Physics, LPD3000, Rhodamine 6G dye, $\Delta E = 0.1$

* Address correspondence to this author. Fax: (+81)75-753-4065. E-mail: baba@kuchem.kyoto-u.ac.jp.

10.1021/jp060563i CCC: $33.50 © 2006 American Chemical Society
Published on Web 07/29/2006

TABLE 1: Vibrational Energies and Assignments of the Bands Observed in the Fluorescence Excitation Spectrum of the S_1 $^1A_1(\pi\pi^*) \leftarrow S_0$ Transition

band no.	vibrational energy (cm^{-1})	band type	assignment
1	0	B	0_0^0 (33 644 cm^{-1})
2	209	B	20_0^1 (a_1)
3	410	A	57_0^1 (b_2)
4	443	A	55_0^1 (b_2)
/5	458	A	56_0^1 (b_2)
6	516	A	38_0^1 (b_1)57_0^1 (b_2)
7	548	A	38_0^1 (b_1)55_0^1 (b_2)
8	561	A	38_0^1 (b_1)56_0^1 (b_2)
9	649	A	20_0^1 (a_1)56_0^1 (b_2)
10	690	A	54_0^1 (b_2)
11	707	B	17_0^1 (a_1)
12	711	A	
13	832	B	16_0^1 (a_1)
14	848	A	
15	857	A	
16	863	A	
17	872	A	
18	876	A	
19	899	A	20_0^1(a_1)54_0^1 (b_2)
20	915	B	
21	919	A	
22	975	A	
23	980	B	
24	989	A	
25	1016	A	
26	1049	B	
27	1052	B	
28	1065	B	
29	1071	B	
30	1079	A	
31	1083	A	
32	1090	A	
33	1097	A and B	
34	1101	A	
35	1115		
36	1149	A	
37	1184	A	

cm^{-1}) pumped by an excimer laser (Lambda Physics LPX 105i, 10 Hz, 150 mJ). UV light was obtained by the second harmonic generation using a BaB_2O_4 crystal. This laser beam intersected the supersonic jet at right angles. The distance between the nozzle and the intersection point was 10 mm. Fluorescence was collected using a lens and detected by a photomutiplier tube (Hamamatsu, R928) through a color filter (Toshiba, UV33) to block the scattered laser light.

The integrated fluorescence intensity was obtained using a boxcar integrator (Stanford Research, SR 250). The fluorescence excitation spectrum was produced by recording the intensity as a function of the laser light wavelength. The energy of a UV laser pulse was approximately 1 mJ. The dispersed fluorescence spectrum was observed using a monochromator (Nikon P250) with a resolution of 30 cm^{-1}.

Result and Discussion

Figure 1 shows the structure and rotational axes of the dibenzofuran molecule. The fluorescence excitation spectrum of dibenzofuran in the supersonic jet for the $S_1 \leftarrow S_0$ transition is shown in Figure 2. The 0_0^0 band is located at 33 644 cm^{-1} and many vibronic bands have high intensities. We identify the vibronic bands by assigning consecutive numbers. Some vibronic bands identified as hot bands changed the relative intensity with a decrease in the pressure of Ar gas. We did not give the band numbers for the hot bands. The excess energies

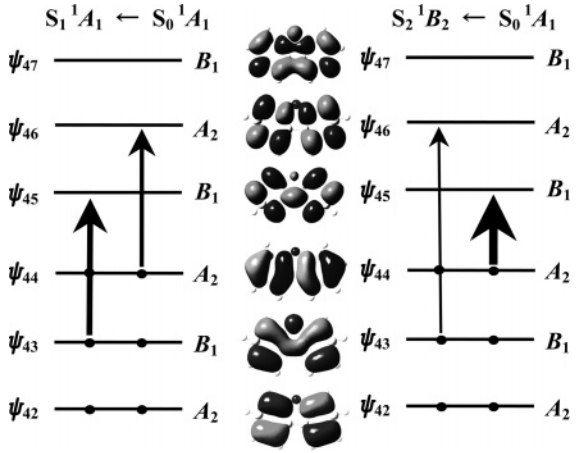

Figure 3. Calculated molecular orbitals and S_1 $^1A_1$ ($\pi\pi^*$) $\leftarrow$ S_0 and S_2 $^1B_2$ ($\pi\pi^*$) $\leftarrow$ S_0 transitions.

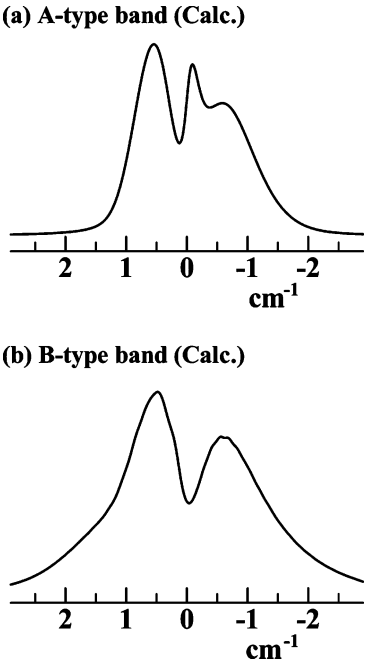

Figure 4. Rotational envelopes for (a) A-type and (b) B-type bands calculated at the resolution of 0.1 cm^{-1} using the rotational constants of $A'' = 0.075\,989$, $B'' = 0.020\,047$ and $C'' = 0.015\,867$ cm^{-1} for the S_0 state and $A' = 0.075\,277$, $B' = 0.019\,831$ and $C' = 0.015\,694$ cm^{-1} for the S_1 state and the rotational temperature of 10 K.

of the observed vibronic bands relative to the 0_0^0 band are summarized in Table 1. To assign these bands, we use symmetry considerations and perform ab initio calculations.

In our recent study on ultrahigh-resolution spectroscopy, the dibenzofuran molecule is shown to be planar in both the S_0 and S_1 states.[8] The transition moment is along the 2-fold symmetry axis of the molecule (z) and the S_1 state is identified as the $^1A_1$ ($\pi\pi^*$) state. The 0_0^0 band of the $S_1 \leftarrow S_0$ transition is the B-type band. In contrast, we find a strong peak of Q transitions near the center of the $0_0^0 + 443$ cm^{-1} band. This is the A-type band, and the transition moment is along the y axis, which is the in-plane long axis. It is assumed that the intensity of this band arises from vibronic coupling with another excited state. As shown later, the $0_0^0 + 443$ cm^{-1} band is assigned to the transition to the $v' = 1$ level of ν_{55} (b_2), which is described as 55_0^1.

First, we consider the vibronic interaction in the dibenzofuran molecule. The vibronic wave function in the Born−Oppenhei-

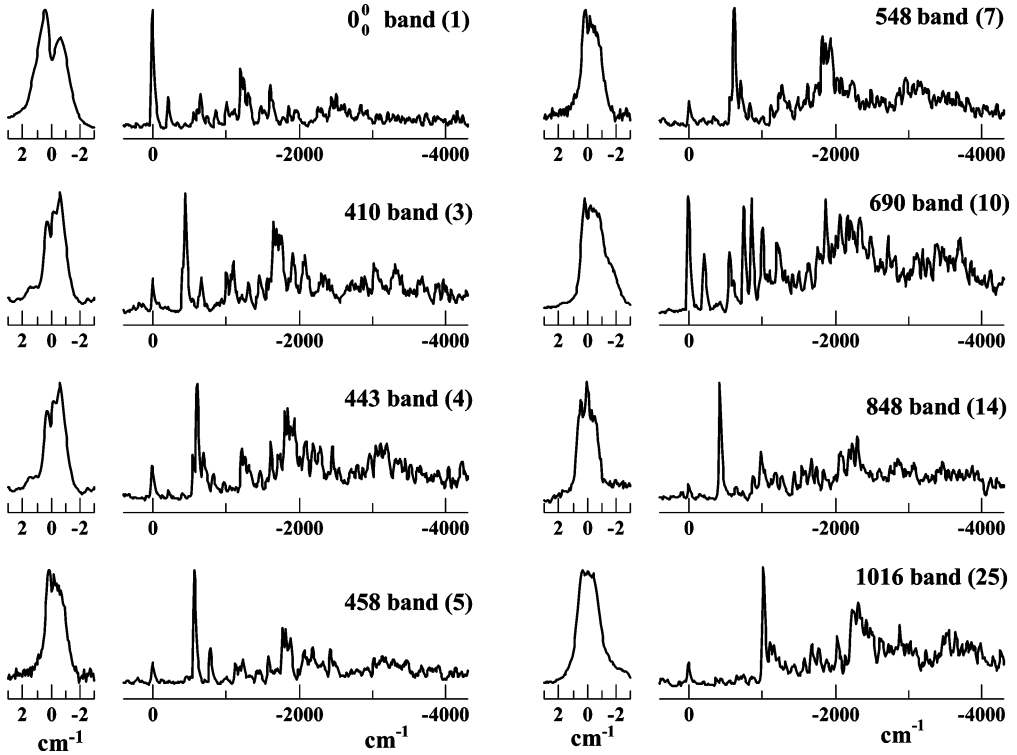

Figure 5. Rotational envelopes of fluorescence excitation spectra and dispersed fluorescence spectra for prominent vibronic bands of the $S_1\ ^1A_1$ ($\pi\pi^*$) ← S_0 transition. For example, "209 band (2)" indicates the $0_0^0 + 209\ cm^{-1}$ band (band number 2).

mer approximation is expressed as follows

$$\Psi_{e\upsilon}(q,Q) = \psi_e(q,Q)\phi_{e\upsilon}(Q) \quad (1)$$

where q and Q denote the electron and vibrational normal coordinates, respectively. $\psi_e(q,Q)$ is the electronic wave function of the e electronic state, and $\phi_{e\upsilon}(Q)$ is the vibrational wave function of the υth vibrational level. The electronic transition moment for the e′ ← e″ electric-dipole transition is given by

$$M_{e'-e''}(\upsilon',\upsilon'') = \langle \Psi_{e'\upsilon'}|\mu|\Psi_{e''\upsilon''}\rangle = \langle \phi_{e'\upsilon'}(Q')|\mu_{e'-e''}(Q'')|\phi_{e''\upsilon''}(\langle Q''\rangle) \quad (2)$$

This can be expanded in the Taylor series of the ith normal mode around the minimum geometry Q'' in the e″ state,

$$\mu_{e'-e''}(Q'') \approx \mu_{e'-e''}(Q_0') + \sum_i \frac{\partial \mu_{e'-e''}}{\partial Q_i}(Q_i'' - Q_{0i}'') + ... \quad (3)$$

where Q_i is the normal coordinate of the ith mode. In the strong allowed dipole transition, the intensity of the vibronic band is calculated using only the first term, which is termed as the Franck−Condon approximation[12−14] and

$$M_{e'-e''}^{FC} = \mu_{e'-e''}(Q''_0)\langle \phi_{e'\upsilon'}(Q')|\phi_{e''\upsilon''}(Q'')\rangle \quad (4)$$

The absorption intensity of the vibronic band is proportional to the square of the transition moment and Franck−Condon factor, $|\langle \phi_{e'\upsilon'}(Q')|\phi_{e''\upsilon''}(Q'')\rangle|^2$.

In the forbidden transition or weak dipole transition, the second term contributes to the absorption intensity of the vibronic band. The truncation after the second term is represented by the Herzberg−Teller (HT) approximation.[15,16] The transition moment is given by

$$M_{e'-e''}^{HT} = \sum_i \frac{\partial \mu_{e'-e''}}{\partial Q_i}\langle \phi_{e'\upsilon'}(Q')|(Q_i'' - Q_{0i}'')|\phi_{e''\upsilon''}(Q'')\rangle \quad (5)$$

It arises from the mixing of the electronic excited states by the vibronic interaction. This is "intensity borrowing" from the other allowed electronic transitions. The vibronic interaction originates from the breakdown of the Born−Oppenheimer approximation, i.e., the interaction between nuclear displacements and electrons. In this case, the direct product of the symmetry species of the electronic wave functions of the borrowing (m) and lending (n) states should be the same as the symmetry species of the induced mode Q_i in C_{2v}:

$$\Gamma(\phi_e^{(m)}) \otimes \Gamma(\phi_e^{(n)}) = \Gamma(Q_i) \quad (6)$$

The HT approximation is valid in most cases and theoretical calculations have been performed for aromatic molecules,[17−21] although quantitative treatments of the adiabatic interaction are required in the strong coupling case.[22,23]

We consider the electronic excited states and vibronic interaction in dibenzofuran. We perform the theoretical calculations of molecular orbitals and allowed electronic transitions using Gaussian 03 program package.[24] The results are shown in Figure 3. The S_1 state is identified as the $^1A_1(\pi\pi^*)$ state by ultrahigh-resolution spectroscopy.[8] There are two configurations of the $^1A_1$ state ψ_{44}(HOMO) → ψ_{46}(LUMO + 1) and ψ_{43}(HOMO − 1) → ψ_{45}(LUMO). These two excited states of the same symmetry species are mixed by configuration interaction and the energies change remarkably. The energy of one of the mixed states becomes less than that of the state of the ψ_{44}(HOMO) → ψ_{45}(LUMO) excitation, which is the S_2 $^1B_2(\pi\pi^*)$ state. We could not identify the 0_0^0 band of the S_2 ← S_0 transition in the supersonic jet. It is assumed that the strong peak at 41 000 cm^{-1} in the vapor absorption spectrum is attributed to this 0_0^0 band.[2] The energy is approximately 7300

cm^{-1} higher and the absorption intensity is considerably stronger than that of the $S_1 \leftarrow S_0$ transition. The S_1 $^1A_1(\pi\pi^*)$ state is mixed with the S_2 $^1B_2(\pi\pi^*)$ state by the vibronic interaction. Further, b_2 vibronic bands appear in the excitation spectrum of the $S_1 \leftarrow S_0$ transition by the intensity borrowing from the $S_2 \leftarrow S_0$ transition and the level energy decreases.[22,23] This spectral feature is similar to that of the $S_1 \leftarrow S_0$ transition of naphthalene,[25-27] although the symmetry is lower in dibenzofuran. The b_2 vibrational level in the S_1 $^1A_1$ state couples with the S_2 $^1B_2$ state and the intensity of the vibronic band arises. Because the direction of the transition moment is different, we can identify the symmetry of each vibronic band by observing the rotational envelope. It is possible to distinguish between A- and B-type bands even by the observed spectrum using the supersonic jet and a nanosecond pulse laser with a resolution of 0.1 cm^{-1}. We determine the rotational envelopes for the A- and B-type bands, as shown in Figure 4. The A-type band is easily distinguished from the B-type band by the strong *Q* peak near the band center and steeper edges of the *P* and *R* peaks. The observed rotational envelopes are shown in Figure 5, and the transition types of the vibronic bands are summarized in Table 1.

Next, we attempt to assign the vibrational modes for the observed vibronic bands by referring to the results of the ab initio theoretical calculations. We calculated energies of normal vibrations in the S_0 and S_1 states at the levels of B3LYP/6-311G(d,p) and RCIS/6-311G(d,p), respectively, and scaled them by factors of 0.9614 and 0.8970 for the S_0 and S_1 states, respectively, as recommended by Scott and Radom.[28] On the basis of the theoretically calculated vibrational energies and observations of the band types, we could assign several vibronic bands unambiguously.

First, the $0_0^0 + 209$ cm^{-1} band (band number 2) is the B-type band, which is a vibronic band of the a_1 mode. The smallest value in the calculated vibrational energy of the a_1 mode is 206 cm^{-1} of ν_{20}. ν_{20} is a vibrational mode of the symmetric rotation of the two phenyl rings. This value is in good agreement with the observed energy. To confirm the assignment, we must determine the vibrational energy in the S_0 state. We observed the dispersed fluorescence spectrum for the excitation of the 0_0^0 band. The result is shown in Figure 5 and the observed vibrational energies are summarized in Table 3. The 211 cm^{-1} band is assigned to 20_1^0. This value is also in good agreement with the calculated value 212 cm^{-1}. Other B-type bands of 707 and 832 cm^{-1} (band numbers 11 and 13) in the fluorescence excitation spectrum are assigned to 17_0^1 and 16_0^1, respectively. The calculated values are 693 and 825 cm^{-1}, and the error is less than 3%.

However, the observed vibrational energies of the b_2 mode in the S_1 state are not in good agreement with the calculated values. The level energy of the b_2 vibration in the S_1 state is considered to be reduced by the vibronic coupling with the S_2 $^1B_2$ state. On the other hand, the vibrational energy in the S_0 state is expected to be close to the calculated value. To determine the vibrational energies in the S_0 state, we observed the dispersed fluorescence spectra for the excitation of the $0_0^0 + 410$, 443 and 458 cm^{-1} A-type bands (band numbers 3-5), and found prominent bands at the vibrational energies of 443, 610 and 568 cm^{-1}, respectively. Therefore, the $0_0^0 + 410$, 443 and 458 cm^{-1} bands in the fluorescence excitation spectrum are assigned to 57_0^1, 55_0^1 and 56_0^1, respectively. The vibrational energy of ν_{55} in the S_0 state is 610 cm^{-1}, and the calculated value is 605 cm^{-1}. In contrast, the vibrational energy in the S_1 state is 443 cm^{-1}, which is significantly less than the calculated value 586 cm^{-1}. It suggests that the 55_0^1 level is remarkably shifted by the vibronic coupling. It is consisitent with the high intensity of this vibronic band. The observed energy of ν_{56} in the S_0 state agrees with the calculated value within the error of 4%. However, the error is larger than 10% for ν_{57}. Other assignments are not realistic because the vibrational energy of this ν_{57} mode is the smallest in the b_2 vibrations. ν_{57} is a vibrational mode of

TABLE 2: Calculated and Observed Vibrational Energies of Dibenzofuran

symmetry	no.	vibration type	S_0 $^1A_1$[a] calc (obs)[c]	S_1 $^1A_1$[b] calc (obs)[d]
a_1	1	C-H stretch	3078	3025
	2	C-H stretch	3067	3015
	3	C-H stretch	3055	3007
	4	C-H stretch	3046	2990
	5	C-C stretch + C-H bend	1606	1604
	6	C-C stretch + C-H bend	1568	1550
	7	C-C stretch + C-H bend	1462	1437
	8	C-C stretch + C-H bend	1414	1434
	9	C-C stretch + C-H bend	1331	1379
	10	C-C stretch + C-H bend	1282	1284
	11	C-O-C sym stretch	1216	1227
	12	C-H bend	1171	1174
	13	C-H bend	1126	1115
	14	C-H bend	1079	1051
	15	C-H bend	993	963
	16	C-O-C bend + ring deform.	831	825 (832)
	17	ring deform.	729	693 (707)
	18	C-O-C bend + ring deform.	646	630
	19	ring deform.	414	403
	20	rings sym rotation	212 (211)	206 (209)
a_2	21	oop C-H wag.	943	904
	22	oop C-H wag.	907	844
	23	oop C-H wag.	830	776
	24	oop C-H wag.	736	684
	25	oop ring deform.	723	639
	26	oop ring deform.	559	483
	27	oop ring deform.	429	390
	28	antisym butterfly	282	244
	29	ring torsion	146	128
b_1	30	oop C-H wag.	944	905
	31	oop C-H wag.	908	847
	32	oop C-H wag.	832	767
	33	oop C-H wag.	737	699
	34	oop ring deform.	709	646
	35	oop ring deform.	552	501
	36	oop ring deform.	414	343
	37	oop C-O-C wag.	305	287
	38	butterfly	103 (105)	97 (106)
b_2	39	C-H stretch	3078	3022
	40	C-H stretch	3066	3012
	41	C-H stretch	3054	3006
	42	C-H stretch	3045	2990
	43	C-C stretch + ring deform.	1576	1681
	44	C-C stretch + ring deform.	1558	1499
	45	C-C stretch + ring deform.	1445	1468
	46	C-C stretch + ring deform.	1426	1414
	47	C-C stretch + ring deform.	1304	1403
	48	C-H bend	1257	1253
	49	C-O-C antisym stretch	1168	1183
	50	C-H bend	1133	1129
	51	C-H bend	1088	1053
	52	C-H bend	1001	986
	53	ring deform.	980	910
	54	ring deform.	828	761 (690)
	55	ring deform.	605 (610)	585 (443)
	56	ring deform.	546 (568)	527 (458)
	57	rings antisym rotation	505 (443)	506 (410)

[a] Results of the B3-LYP/6-311G(d,p) level are scaled by 0.9614. [b] Results of the RCIS/6-311G(d,p) level are scaled by 0.8970. [c] Determined using the dispersed fluorescence spectra with an accuracy of ± 10 cm^{-1}. [d] Determined using the fluorescence excitation spectra with an accuracy of ± 1 cm^{-1}.

TABLE 3: Vibrational Energies and Assignments of the Bands Observed in the Dispersed Fluorescence Spectrum for the Excitation of the 0_0^0 Band of the S_1 $^1A_1(\pi\pi^*) \leftarrow S_0$ Transition

band no.	vibrational energy (cm^{-1})	assignment
1	0	0_0^0 (33 644 cm^{-1})
2	211	20_1^0 (a_1)
3	568	56_1^0 (b_2)
4	610	55_1^0 (b_2)
5	655	
6	858	
7	1008	
8	1203	
9	1236	
10	1305	
11	1476	
12	1606	
13	1854	
14	1958	
15	2256	
16	2440	
17	2504	
18	2612	
19	2684	
20	2854	

the antisymmetric rotation of the two phenyl rings. Thus, the assignments for these three A-type bands are reliable. The next A-type $0_0^0 + 690$ cm^{-1} band (band number 10) is also unambiguously assigned to 54_0^1.

Thus, we have experimentally determined the vibrational energies of several modes in the S_1 state. Most of the strong bands are identified as the b_2 fundamental bands. Evidently, the weak bands at 516, 548 and 561 cm^{-1} (band numbers 6−8) are the combination bands of the bands at 410, 443 and 458 cm^{-1} (band numbers 3−5) with another mode of 106 cm^{-1}. This small energy is produced by an out-of-plane vibrational mode and is assigned to $\nu_{38}(b_1)$ by referring to the calculated energies. A $b_1 \otimes b_2 = a_2$ vibronic band is symmetry forbidden. The appearance of the combination bands suggests symmetry lowering by molecular distortion. The determined vibrational energies in the S_1 state are summarized in Table 1 together with the calculated ones. The spectrum is congested in the higher energy region and it is not easy to make reliable assignments for the observed vibronic bands.

A broad emission is remarkably observed for the excitation of the high vibrational levels. This suggests interaction with other electronic states. The contribution of the triplet state is expected to be negligibly small on the basis of an analogy of benzene and naphthalene. In these molecules, Zeeman broadening is shown to be very small by ultrahigh-resolution spectroscopy.[29−34] Therefore, the broad emission is attributed to intramolecular vibrational redistribution (IVR), which is considered to occur efficiently in the high vibrational levels of the S_1 state of dibenzofuran. The threshold energy is significntly less than that of naphthalene (2122 cm^{-1})[35] or anthracene (approximately 1800 cm^{-1}).[36,37] It is assumed that the threshold energy decreases due to the low-frequency vibrational modes and low symmetry of the dibenzofuran molecule. The rate of nonradiative transition in a large molecule is given by[38,39]

$$k_{nr} = \left(\frac{2\pi}{\hbar}\right)V^2\rho \qquad (7)$$

where V is the interaction matrix element and ρ is the effective density of coupling levels. It is expected that the level density in the S_1 state of dibenzofuran will be large and it will increase even in the lower energy region because several low-frequency modes exist and the symmetry is lower. Therefore, the IVR threshold energy is less than that of aromatic polyacenes with a similar molecular size.

In summary, the fluorescence excitation spectrum and dispersed fluorescence spectra in which a single vibronic level is excited have been observed and analyzed for the S_1 $^1A_1$ ($\pi\pi^*$) $\leftarrow$ S_0 transition of jet-cooled dibenzofuran. We have also observed the rotational envelopes of the vibronic bands in the excitation spectrum and assigned the observed vibronic bands by referring to the results of theoretical calculations. The b_2 vibronic bands are strongly observed and the intensity is considered to arise from vibronic coupling with the S_2 $^1B_2$ ($\pi\pi^*$) state. Remarkably, a broad emission originating from the IVR is observed for the high vibrational levels in the S_1 state.

Acknowledgment. This study is supported by a Grant-in-Aid for Scientific Research from the Ministry of Education, Culture, Sports, Science, and Technology of Japan. We thank Mr. N. Mizutani, H. Miyashita, and Y. Takamatsu (Equipment Development Center, Institute for Molecular Science) for their assistance in constructing the apparatus.

References and Notes

(1) Baba, M.; Doi, A.; Tatamitani, Y.; Kasahara, S.; Katô, H. *J. Phys. Chem. A* **2004**, *108*, 1388.
(2) Bree, A.; Vilkos, V. V. B.; Zwarich, R. *J. Mol. Spectrosc.* **1973**, *48*, 124.
(3) Bree, A.; Vilkos, V. V. B.; Zwarich, R. *J. Mol. Spectrosc.* **1973**, *48*, 135.
(4) Bree, A.; Lacey, A. R.; Ross, I. G.; Zwarich, R. *Chem. Phys. Lett.* **1974**, *26*, 329.
(5) Taliani, C.; Bree, A.; Zwarich, R. *J. Phys. Chem.* **1984**, *88*, 2357.
(6) Khasawneh, I. M.; Winefordner, J. D. *Talanta* **1988**, *35*, 267.
(7) Klots, T. D.; Collier, W. B. *J. Mol. Struct.* **1996**, *380*, 1.
(8) Yamawaki, M.; Tatamitani, Y.; Doi, A.; Kasahara, S.; Baba, M. *J. Mol. Spectrosc.* **2006**, *238*, 49.
(9) Auty, A. R.; Jones, A. C.; Phillips, D. *J. Chem. Soc., Faraday Trans. 2* **1986**, *82*, 1219.
(10) Weickthardt, C.; Zimmermann, R.; Boesl, U.; Schlag, E. W. *Rapid Commun. Mass Spectrom.* **1993**, *7*, 183.
(11) Chakraborty, T.; Lim, E. C. *Chem. Phys. Lett.* **1993**, *207*, 99.
(12) Franck, J. *Trans. Faraday Soc.* **1925**, *21*, 536.
(13) Condon, E. U. *Phys. Rev.* **1926**, *28*, 1182.
(14) Condon, E. U. *Phys. Rev.* **1928**, *32*, 858.
(15) Herzberg, G.; Teller, E. *Z. Phys. Chem. Abt. B* **1933**, *21*, 410.
(16) Atkins, P. W.; Friedman, R. S. *Molecular Quantum Mechanics*; Oxford University Press: New York, 1997.
(17) Ohno, K. *Chem. Phys. Lett.* **1980**, *70*, 526.
(18) Baranov, V. I.; Gribov, L. A. *J. Mol. Struct.* **1981**, *70*, 31.
(19) Baranov, V. I.; Gribov, L. A.; Djenjer, V. O.; Zelent'sov, D. Y. *J. Mol. Struct.* **1997**, *407*, 199.
(20) Bemhardsson, A.; Forsberg, N.; Malmqvist, P.; Roos, B. O.; Serrano-Andrés, L. *J. Chem. Phys.* **2000**, *112*, 2798.
(21) Dierksen, M.; Grimme, S. *J. Phys. Chem. A* **2004**, *108*, 10225.
(22) Fulton, R. L.; Gouterman, M. *J. Chem. Phys.* **1961**, *35*, 1059.
(23) Fulton, R. L. *J. Chem. Phys.* **1972**, *56*, 1210.
(24) Frisch, M. J.; Trucks, G. A.; Schlegel, H. B.; Scuseria, G. E.; Robb, M. A.; Cheseman, J. R.; Montgomery, J. A., Jr.; Vreeven, T.; Kudin, K. N.; Burant, J. C.; Millam, J. M.; Iyengar, S. S.; Tomasi, J.; Barone, V.; Mennuci, B.; Cossi, M.; Scalmani, G.; Rega, N.; Petersson, G. A.; Nakatsuji, H.; Hada, M.; Ehara, M.; Toyota, K.; Fukuda, R.; Hasegawa, J.; Ishida, M.; Nakajima, T.; Honda, Y.; Kitao, O.; Nakai, H.; Klene, M.; Li, X.; Knox, J. E.; Hratchian, H. P.; Cross, J. B.; Adamo, C.; Jaramillo, J.; Gomperts, R.; Stratmann, R. E.; Yazyev, O.; Austin, A. J.; Cammi, R.; Pomelli, C.; Ochtersky, J. W.; Ayala, P. Y.; Morokuma, K.; Voth, G. A.; Salvador, P.; Dannenberg, J. J.; Zakrzewski, V. G.; Dapprich, S.; Daniels, A. D.; Strain, M. C.; Farkas, O.; Malick, D. K.; Rabuck, A. D.; Raghavachari, K.; Foresman, J. B.; Ortiz, J. V.; Cui, Q.; Baboul, A. G.; Clifford, S.; Cioslowski, J.; Stefanov, B. B.; Liu, G.; Liashenko, A.; Piskorz, P.; Komaromi, L.; Martin, R. L.; Fox, D. J.; Keith, T.; Al-Laham, M. A.; Peng, C. Y.; Nanayakkara, A.; Challacombe, M.; Gill, P. M. W.; Johnson, B.; Chen, W.; Wong, M. W.; Gonzalez, C.; Pople, J. A. *Gaussian 03*, revision B.05; Gaussian, Inc.: Pittsburgh, PA, 2003.
(25) Beck, S. M.; Powers, D. E.; Hopkins, J. B.; Smalley, R. E. *J. Chem. Phys.* **1980**, *73*, 2019.

(26) Behlen, F. M.; McDonald, D. B.; Sethuraman, V.; Rice, S. A. *J. Chem. Phys.* **1981**, *75*, 5685.
(27) Joo, D. L.; Takahashi, R.; O'Reilly, J.; Katô, H.; Baba, M. *J. Mol. Spectrosc.* **2002**, *215*, 155.
(28) Scott, A. P.; Radom, L. *J. Phys. Chem.* **1996**, *100*, 16502.
(29) Doi, A.; Kasahara, S.; Katô, H.; Baba, M. *J. Chem. Phys.* **2004**, *120*, 6439.
(30) Wang, J.; Doi, A.; Kasahara, S.; Katô, H.; Baba, M. *J. Chem. Phys.* **2004**, *121*, 9188.
(31) Baek, D. Y.; Wang, J.; Doi, A.; Kasahara, S.; Katô, H.; Baba, M. *J. Phys. Chem. A* **2005**, *109*, 7127.
(32) Baek, D.; Chen, J.; Wang, J.; Doi, A.; Kasahara, S.; Baba, M.; Katô, H. *Bull. Chem. Soc. Jpn.* **2006**, *79*, 75.
(33) Okubo, M.; Misono, M.; Wang, J.; Baba, M.; Katô, H. *J. Chem. Phys.* **2002**, *116*, 9293.
(34) Okubo, M.; Wang, J.; Baba, M.; Misono, M.; Kasahara, S.; Katô, H. *J. Chem. Phys.* **2005**, *122*, 144303−1.
(35) Beck, S. M.; Hopkins, J. B.; Powers, D. E.; Smalley, R. E. *J. Chem. Phys.* **1981**, *74*, 43.
(36) Lambert, W. R.; Felker, P. M.; Zewail, A. H. *J. Chem. Phys.* **1984**, *81*, 2209.
(37) Amirav, A.; Horwitz, C.; Jortner, J. *J. Chem. Phys.* **1988**, *88*, 3092.
(38) Bixon, M.; Jortner, J. *J. Chem. Phys.* **1968**, *48*, 715.
(39) Avouris, P.; Gelbart, W. M.; El-Sayed, M. A. *Chem. Rev.* **1977**, *77*, 793.